



Research article

The role of FGF-21 in promoting diabetic wound healing by modulating high glucose-induced inflammation

Zheling Li ^{a,1}, Xiaohui Qiu ^{a,1}, Gaopeng Guan ^b, Ke Shi ^a, Shuyue Chen ^a, Jiangjie Tang ^c, Muzhang Xiao ^d, Shijie Tang ^e, Yu Yan ^{a,b}, Jianda Zhou ^{a,*}, Huiqing Xie ^{f,**}

^a Department of Plastic and Reconstructive Surgery, Xiangya III Hospital of Central South University, Changsha City, People's Republic of China

^b Department of Endocrinology, Xiangya III Hospital of Central South University, Changsha City, People's Republic of China

^c Department of Stomatology, Xiangya III Hospital of Central South University, Changsha City, People's Republic of China

^d Department of Plastic and Cosmetic Surgery, Xiangya Hospital, Changsha, Hunan, People's Republic of China

^e Department of Plastic and Cosmetic Surgery, Second Affiliated Hospital of Shantou University Medical Collage, Shantou City, People's Republic of China

^f Department of Rehabilitation Medicine, Xiangya III Hospital of Central South University, Changsha City, People's Republic of China

ARTICLE INFO

Keywords:

Fibroblast growth factor 21 (FGF-21)
Diabetic wound healing
Inflammation
Pyroptosis
Endothelial cells

ABSTRACT

Background: Wound healing is a complex biological process that can be impaired in individuals with diabetes. Diabetic wounds are a serious complication of diabetes that require promoting diagnosis and effective treatment. FGF-21, a member of the endocrine FGF factors family, has caught the spotlight in the treatment of diabetes for its beneficial effects on accelerating human glucose uptake and fat catabolism. However, the therapeutic efficacy of FGF-21 in promoting diabetic wounds remains unknown. This study aims to evaluate the therapeutic potential of FGF-21 in promoting diabetic wound healing.

Methods: we investigated the effects of FGF-21 on wound healing related-cells under high-glucose conditions using various assays such as CCK8, scratch assay, flow cytometry analysis, endothelial tube-formation assay, and transmission electron microscopy. Furthermore, we used db/db mice to verify the healing-promoting therapeutic effects of FGF-21 on diabetic wounds. We also conducted qRT-PCR, Western blot, and immunofluorescence staining analyses to elucidate the underlying mechanism.

Result: Our results indicate that FGF-21 treatment restored hyperglycemic damage on endothelial cell proliferation, migration, and tube-forming ability. It also reduced endothelial cell death rates under high-glucose conditions. TEM analysis showed that FGF-21 treatment effectively restored mitochondrial damage and morphological changes in endothelial cells caused by glucose. Additionally, qRT-PCR and Western blot analysis indicated that FGF-21 treatment restored inflammatory responses caused by hyperglycemic damage. Animal experiments confirmed these findings, suggesting that FGF-21 may be a promising candidate for the treatment of non-healing diabetic wounds due to its effectiveness in stimulating angiogenesis and anti-inflammatory function.

* Corresponding author. Department of Plastic and Reconstructive Surgery, Xiangya III Hospital of Central South University, 138 tongzipo Road 410000, Changsha City, People's Republic of China.

** Corresponding author.

E-mail addresses: 2643086276@qq.com (Y. Yan), zhoujianda@csu.edu.cn (J. Zhou), xiaoxiang0733@126.com (H. Xie).

¹ Zheling Li and Xiaohui Qiu contributed equally to this work.

<https://doi.org/10.1016/j.heliyon.2024.e30022>

Received 22 May 2023; Received in revised form 18 April 2024; Accepted 18 April 2024

Available online 28 April 2024

2405-8440/© 2024 Published by Elsevier Ltd.

This is an open access article under the CC BY-NC-ND license

(<http://creativecommons.org/licenses/by-nc-nd/4.0/>).

Conclusion: Our study provides evidence that FGF-21 is an essential regulator of wound-related cells under high-glucose conditions and has the potential to be a novel therapeutic target for accelerating diabetic wound healing.

1. Introduction

Wound healing is a complex and dynamic physiological process, including four main phases: Hemostasis, inflammation, proliferation, re-epithelialization, and remodeling [1]. However, complicated by underlying conditions such as persistent inflammation, peripheral angiopathies, associated neuropathy, impaired secretion or function of matrix metal loproteinases (MMPs), increasing in reactive oxygen species, it always remain impaired under diabetes conditions and promoting the occurrence of chronic wounds [2–5]. Among the major chronic wounds, including pressure and venous ulcers, diabetic foot ulceration (DFU), occurring in about 20 % of diabetic population, has become one of the most frequent complications of diabetes [6]. Due to its slow healing process, recurrent cycles of reinfection, and debilitating complications, this condition has posed a severe public health problem [7,8].

The diabetic wound healing process requires the coordinated behaviors of numerous cells types, especially proliferation, migration, and ability of vascularization of wound healing-related cells [9]. Multiple factors, including growth factors, cytokines, and antimicrobial peptides, are needed to interact and stimulate endothelial cells, fibroblast, and keratinocytes to proliferate and migrate into wound sites [10,11]. Despite this, the fundamental processes underlying wound healing in people with long-term diabetes remain unclear [12]. Diabetic ulcers are persistently difficult to heal due to the interplay of multiple factors. Among them, macrophage function is impaired at wound sites, resulting in decreased release of cytokines such as TNF- α and IL-1 β . Simultaneously, a high glucose environment leads to the deformation and dysfunction of essential cells involved in healing, such as epithelial cells, fibroblasts, and keratinocytes. These factors collectively promote a pro-inflammatory state within diabetic wounds, causing delayed healing. Ultimately, these complex interactions contribute to the formation of chronic, non-healing diabetic ulcers [13].

Thus, a better understanding of the molecules regulating the function and behaviors of wound healing-related cells prolonged exposure to hyperinsulinemia or hyperglycemia would provide insight into the process and treatment of diabetic wounds.

Numerous studies have suggested that the application of exogenous growth factors (GFs) is a promising therapeutic approach for treating chronic, refractory wounds. GFs play a key role by initiating and coordinating various cellular and molecular events, including the induction of vascular endothelial GF (VEGF), fibroblast GF (FGF), hepatocyte GF, epidermal GF (EGF), transforming GF- β (TGF- β), angiopoietin, and cytokines such as TNF- α . These factors contribute to the stimulation of angiogenesis, which is essential for successful tissue healing by promoting accumulation at the site of inflammation [14].

Previous research has suggested that vascular endothelial growth factor (VEGF) is the most effective promoter of angiogenesis during wound healing and is currently the most commonly used growth factor in chronic wound treatment [15]. While, a recent study confirmed that fibroblast growth factor (FGF) has a more potent angiogenic effect than other growth factors such as platelet-derived growth factor (PDGF) and vascular endothelial growth factor (VEGF), stimulating angiogenesis and fibroblast proliferation to form granulation tissue [16]. FGF is secreted in a paracrine or endocrine manner [17], with FGF-21 being of particular interest due to its beneficial effects on obesity, diabetes mellitus, glucose and lipid metabolism, cardiovascular stress damage prevention, and accelerated human glucose uptake and energy metabolism [18,19]. Taken together, these results lead us to speculate that FGF-21 may play a more essential role in promoting diabetic wound healing because of its unique advantages over other types of growth factors.

Pyroptosis is a recently found endogenous cell death process characterized by persistent swelling and expansion of cells until the cell membrane ruptures, resulting in the release of cellular contents and the activation of an inflammatory response [19]. Pyroptosis is characterized by activation of the NLRP3 inflammasome, caspase activation, formation of pore on the cell membrane, and the release of interleukin-1 β (IL-1 β) and interleukin-18 (IL-18) [20]. Recently, using γ -tocotrienols to inhibit the activation of the NLRP3 inflammasome, thereby reducing caspase-1 cleavage and IL-1 β release in macrophages, has been reported to achieve the goal of delaying the progression of type 2 diabetes mellitus (T2 DM) [21]. In addition, there is growing evidence that inhibition of the pyroptosis pathway could control the development of related diabetes-associated complications [22,23]. Furthermore, FGF-21 levels are strongly associated with hyperglycemia exposure in multiple tissues, including the liver, adipose tissue, and heart [24]. However, the function of FGF-21 in diabetic wound repair still remains poorly understood.

In this study, we aimed to determine whether FGF-21 contributes to the proliferation, migration, cell pyroptosis, and vascularization ability of endothelial cells during the diabetic wound healing process. Using db/db mice model, we found that FGF-21 displayed similar angiogenic effects to VEGF and had stronger anti-inflammatory effects than VEGF in the context of diabetic wound healing.

2. Materials and methods

HUVEC and NIH-3T3 cells were tested separately in a series of in vitro functional assays to determine the effect of FGF-21 on endothelial cells and fibroblasts in a high glucose environment. And for in vivo experiments, we used db/db mice to perform several animal and histological analyses.

2.1. Cell culture

HUVEC and NIH-3T3 cells were obtained from (Procell Life Science & Technology co, Wuhan, China). Specifically cultured NIH-

3T3 and HUVEC cell in Dulbecco's Modified Eagle Medium (DMEM, Gibco, USA) and Dulbecco's Modified Eagle Medium/Nutrient Mixture F12 Medium (DMED/F12, Biosharp, China). 10 % fetal bovine serum (FBS, Biosharp, China), 100 μ /ml penicillin, and 100 μ g/ml streptomycin were supplemented for cell. Cell cultures were maintained at 37 °C in a humidified atmosphere of 5 % CO₂. All cells were divided into three groups for living conditions: 30 mM glucose, 30 mM glucose+200 ng/ml FGF-21 (Novoprotein, China), and control. In the control group, no ingredients other than basal medium were added.

2.2. Cell counting Kit-8 assay (CCK8)

Cells in three groups mentioned above were seeded into a 96-well at a density of 2000 cells per well. After 24, 48, 72 and 96 h, added 10 μ L of CCK8 solution into each well and maintained plates at 37 °C for another 2 h. The cells were detected by an enzyme labeling instrument (Thermo Fisher Scientific, USA) with a wavelength of 450 nm.

2.3. Scratch test

HUVEC cells were suspended in a 900 μ L medium and seeded at a concentration of 5×10^5 on a 6-well plate. When the confluence reached about 70–80 %, three even lines were drawn in each well by a 1000 μ L pipette tip. The cells were washed for three times with PBS (1 ml). Then, serum-free medium was added and cultured at 37 °C in 5 % CO₂ for 24 and 48 h, at which photos were taken. The same intervention was applied to three replicate wells, resulting in a total of nine wells in the scratch assay. The healing rate was calculated by the following formula: Cell migration rate % = (1 - scratch area/original scratch area) \times 100.

2.4. Flow cytometry for apoptosis assay

HUVEC cells were grouped as above mentioned. According to the protocol of a FITC-Annexin V cell apoptosis assay kit (BD Biosciences). Normal cultured and induced apoptosis cells ($0.5\text{--}1 \times 10^6$), 100 μ L of staining buffer and FITC-labeled Annexin V (20 μ g/mL) of 10 μ L were added, and the cells were protected from light for 30 min at room temperature. Propidium iodide double-stained the cells (put in room temperature for 5 min). Then the cells were analyzed using a flow cytometer (FACScan; BD Biosciences, American, USA). The total apoptotic cell rate was calculated as follows:

Early apoptotic cell rate (LR, lower right quadrant-prophase apoptosis) + late apoptotic cell rate (UR, upper right quadrant-advanced stage apoptosis).

2.5. Endothelial tube-forming assay

Cells were cultured in 3 groups, as mentioned above. Each group consisted of three replicate wells, totaling nine wells. HUVEC was seeded in 96-well plates at a density of $2\text{--}3 \times 10^4$ and was precooled with 50 μ L Matrigel (Biosharp, China) per well (the matrix gel was thawed at 4 °C and mixed uniformly by using cooled pipette tips) and incubated for 1 h at a cell incubator. Then added 50 μ L culture medium to each well and set the plates at 37 °C for 18 h. All operations need to be careful to avoid bubbles. Finally, observe the plates after staining endothelial tubes with Calcein AM dye. Five visual fields were randomly chosen under a $100 \times$ fluorescent microscope to observe and count the endothelial cells.

2.6. Transmission electron microscope cell morphology observation (TEM)

HUVEC (1×10^5 cells/well) were co-cultured in 6 different medium environments. Specifically, there are six groups: DMEM plus PBS, DMEM plus 30 mM glucose, DMEM plus 30 mM glucose and 200 ng/ml FGF-21 (Beyotime Recombinant Human FGF-21), DMED plus 60 mM glucose, and DMED plus 60 mM glucose and 400 ng/ml FGF-21. The cell morphology was observed under the transmission electron microscope (Philips CM10, Netherlands).

2.7. RNA isolation and quantitative real-time PCR (qRT-PCR)

After 48 h of culture, the HUVEC cells were grown on a 6-well plate and grouped as described above. RNA was extracted using the cell/tissue miRNA extraction Kit (Vazyme Biotech Co, China). There were 3 groups of cells, with each group containing 3 replicate wells, resulting in a total of 9 original RNA samples extracted. Nanodrop was used to determine the concentration of extracted RNA. Afterward, using the HiFiScript cDNA Synthesis Kit (Vazyme Biotech Co, China). According to the manufacturer's instruction, in a 100- μ L volume, 500 ng RNA was used per cDNA reaction complementary DNA (cDNA) was synthesized from 1 mg of RNA. The qPCR were performed in 20- μ L reaction volumes with 500 nM forward primer and 500 nM reverse primer for the 4- μ L cDNA, with fluorescence acquisition performed at the annealing step, on a Roche-Gene Q PCR machine (Roche LightCycler480II, USA).

2.8. LDH assay

The LDH levels of 9 wells of cells from 3 groups are measured as follows: 48 h of co-culture using LDH activity kits (Beyotime, Shangsha, China). Cell supernatant was collected and processed as directed by the manufacturer protocol. The absorbance of each well was measured at 490 nm to determine the LDH activity.

2.9. Western blotting analysis

Cells were obtained from the three groups mentioned above. All cells were lysed with RIPA lysis buffer (Biosharp, Anhui, China) containing 1 % PMSF (Biosharp, Anhui, China). BCA protein assay kit (Biosharp, Anhui, China) were used to test the protein concentration. The sample of cell lysates were boiled for about 10min. Those proteins were subjected to 10 % gel electrophoresis and then transferred to polyvinylidene fluoride membranes. The membranes incubated at 4° overnight with primary Ab against and then incubated with secondary AB against. Finally, The membranes were exposed in PVDF film after dripping ECL luminous solution. The strength of the signal is measured and analyzed by Image J.

2.10. Ethical statement, animal care, and wound healing rate assay

Animal Laboratory of the Third Xiangya Hospital (Central South University) provided 30 ten-week-old male db/db mice (Changsha, China). All related animals conformed to the guidelines for Animal Care and Use of the Animal Laboratory of the Third Xiangya Hospital (Central South University). The protocols and procedures reached the permission of the Ethics Committee of XiangYa Medical College (CSU-2022-0398).

We spend one week for the mice to adapt to the environment, placing all the db/db mice (weighing 45–55g, aged 6–8 weeks) in a specific pathogen-free (SPF) environment, which was maintained at constant temperature (22 ± 2 °C) and humidity (40%–60 %) with a 12/12 h dark-light cycle (lights on at 7:00 a.m.). After the mice have become acquainted with their environment, we create two 1 cm diameter wounds on each mouse's buttocks. The 30 db/db mice were divided into 3 group: NS group (subcutaneous injection 0.5 ml 0.9 % NaCl under the wound), FGF-21 group (injection of 5ug/kg FGF-21 under the wound) and VEGF group (subcutaneous injection of 5ug/kg VEGF). The wound Healing rate = (original wound area - current measured area) ÷ original wound area × 100 %.

2.11. H&E, Masson and immunohistochemical staining

H&E and Masson staining were carried out for histomorphological analysis: On day 11 of the animal experiment, the wound tissue was excised and fixed in formalin. After being paraffin-embedded, the specimen was stained with hematoxylin and eosin (H&E) or Masson's trichrome (Sigma Aldrich). Serial sections in 4 μm thickness were mounted on slides. H&E and Masson-stained section images were obtained from sequential fields with a plan apochromatic objective (× 1000) and Image J software was used to analyze the figure.

Immunohistochemical staining: Tissue was collected from the NS, VEGF, and FGF-21 groups, fixed with 10 % formalin for 24 h and embedded in paraffin wax. The tissues were sliced 4 μm thick and then processed following the instructions of the Streptomyces Habilis Ovalbumin-Biotin Kit (ZSGB-BIO, China) and were stained by NF-κB p65, IL-1β, NLRP3, CD31 antibody (Proteintech, 1/100-1/200, dilution) and following the manufacturer's instructions. The slides were scanned using a 3DHitech Panoramic 250 Flash II slide scanner. Images were obtained under a microscope after dehydration and adjusting transparency. Images analyzed by Image J software (Within the same group, there are 3 stained slides with the same treatment purpose)

2.12. Enzyme-linked immunosorbent assay (ELISA)

This experiment was carried out using the ELISA Kits (Thermo Fisher, USA). We collected the wound tissue (NS, VEGF, and FGF-21 groups). According to the Kits' instructions, they lysed the tissue. The tissues were centrifuged at 2–8 °C for 10 min at 300×g, and the supernatant fraction was collected for analysis. 100 μl of antibody dilutions and supernatant samples were used per well. Then incubated at 37 °C for 1 h and incubated with substrate solution at 37 °C for 15 min. Adding the stop solution terminated the reaction. Finally, according to the manufacturer's instructions, the sample's OD value at 450 nm wavelength was measured using a microreader (Thermo Fisher, USA). Drawing the standard curve used the GraphPad Prism 5 software and calculated the concentration of each sample (The supernatant from 9 samples in 3 groups is being tested.)

2.13. TUNEL assay

The TUNEL assay for assessing animal tissue apoptosis was performed using a One-Step TUNEL Apoptosis Assay kit (Thermo Fisher, USA). We collect the tissue from NS, VEGF, and FGF-21 groups. The wound tissue was fixed with 4 % paraformaldehyde. The TUNEL

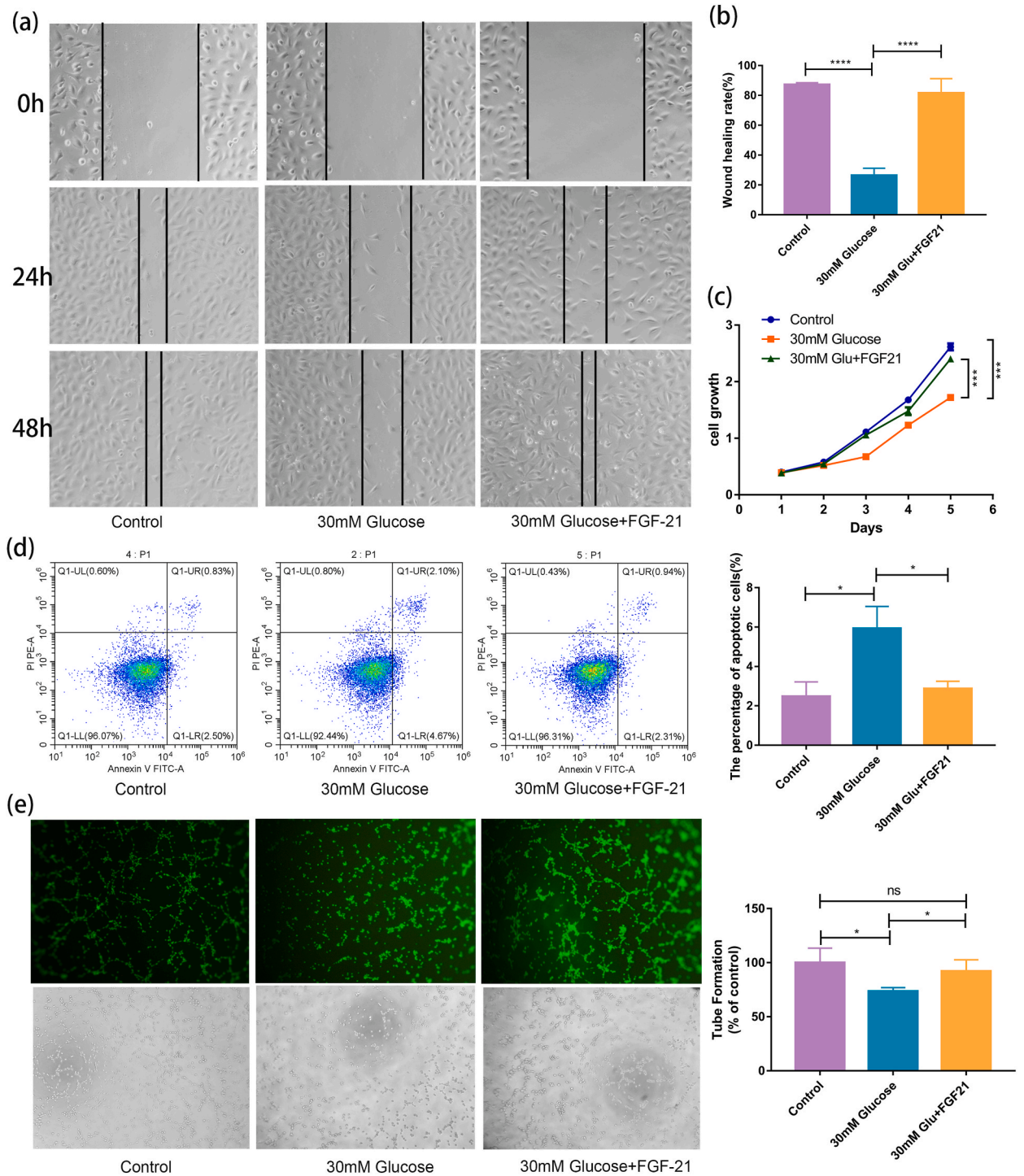


Fig. 1. FGF-21 restores cell function in high glucose condition. (c) Effects of Glucose and FGF-21 on cell proliferation of HUVEC, measured via the CCK8 assay; (a) Migration properties of HUVEC cells treated with either 30 mM Glucose or 30 mM Glucose + FGF-21 were determined in the scratch assay. Magnification: $\times 100$; (b) Quantification result of scratch assay; (d) Flow cytometry analysis of HUVEC cells treated with either 30 mM Glucose or 30 mM Glucose + FGF-21 and statistical result of flow cytometry analysis; (e) The tube formation assay and Quantification result. (ns: $P > 0.05$; * $P < 0.05$; ** $P < 0.01$).

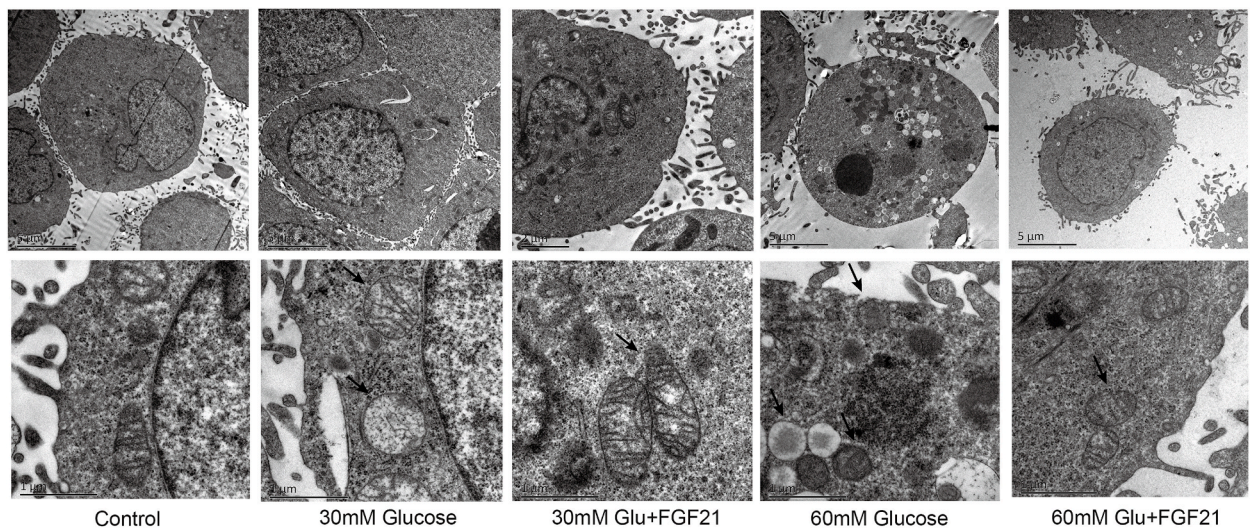
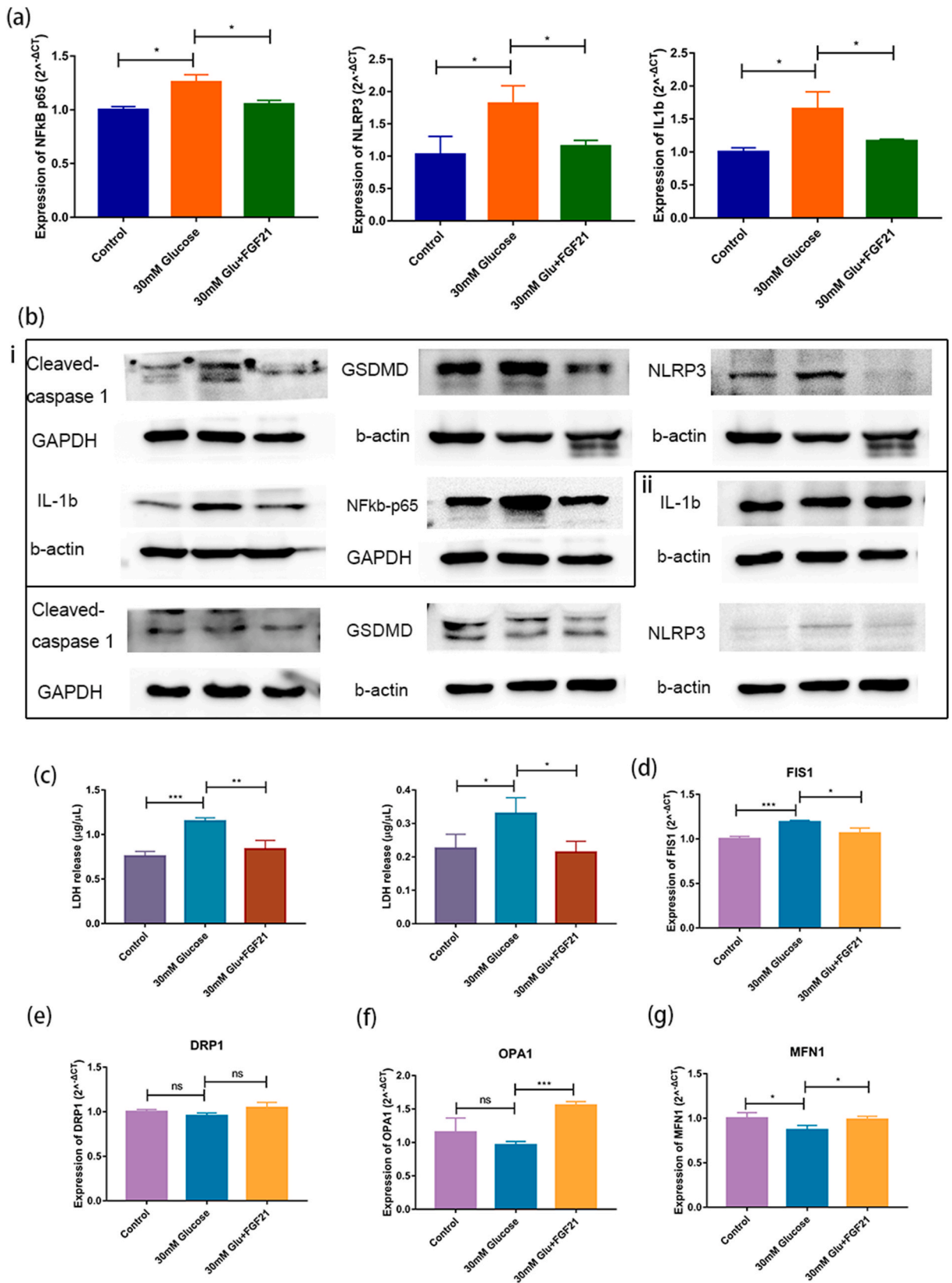


Fig. 2. The morphological changes in endothelial cells under high glucose conditions (30 mM and 60 mM) were reversed by FGF-21, detected by TEM.



(caption on next page)

Fig. 3. FGF-21 inhibited high glucose-induced pyroptosis activation in vitro. (a) The mRNA expression level of NF- κ B p65, NLRP3 and IL-1 β in endothelial cells (control, 30 mM glucose and 30 mM glucose + FGF-21 group); (b) Western blot results of pyroptosis indicators in endothelial cells and NIH-3T3 cells; (c) LDH release assay of endothelial cells and NIH-3T3 cells in different group; (d) The mRNA levels of FIS1, (e) The mRNA levels of DRP1, (f) The mRNA levels of OPA1, and (g) The mRNA levels of MFN1. Endothelial cells treated with 30 mM glucose or glucose + FGF-21, as measured by qRT-PCR. (ns: $P > 0.05$; * $P < 0.005$; ** $P < 0.01$; *** $P < 0.001$).

staining reagent and DAPI dye were then employed to stain the cells, and three randomly selected visual fields were examined under a fluorescence microscope.

2.14. Statistic and analysis

The studies were conducted in triplicate, and the results were evaluated with the Student's t-test and represented as mean \pm SD. Differences were considered significant at $p < 0.05$.

3. Results

3.1. FGF-21 restores HUVEC cell function and proliferative capacity under high glucose stress

The scratch test was initially employed to measure the migration rate in the HUVEC cell line to study the link between FGF-21 and wound healing-related cell lines in a high glucose environment. The migration rate of the 30 mM glucose group is $24.52 \% \pm 4.22 \%$, significantly lower than the control group's migration rate of $86.13 \% \pm 1.21 \%$; However, upon administration of FGF-21, the wound healing rate was $79.44 \% \pm 8.94 \%$, significantly higher than that of the 30 mM glucose group.

(Fig. 1A–B). The CCK-8 assay was then conducted to assess proliferation in three groups. The CCK-8 cell proliferation results were as follows: control group 2.52 ± 0.49 , 30 mM glucose group 1.63 ± 0.64 , and 30 mM Glu + FGF21 group 2.31 ± 0.35 . The result showed that the addition of 30 mM glucose significantly inhibited HUVEC proliferation, and the proliferative ability of HUVEC inhibited by high glucose was significantly restored with the addition of FGF-21 (Fig. 1C).

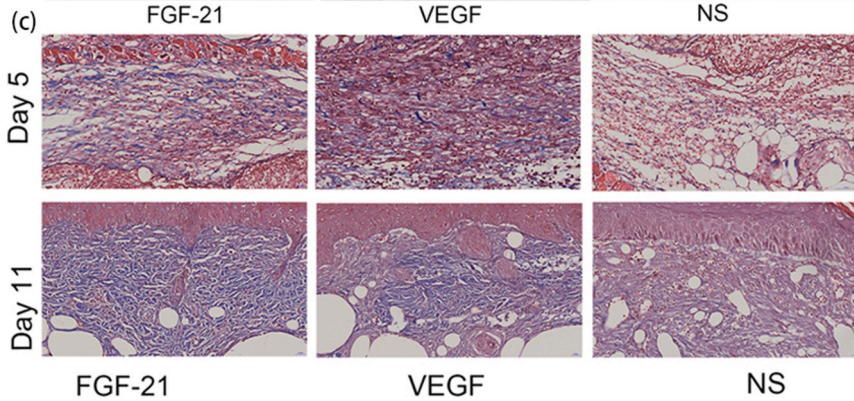
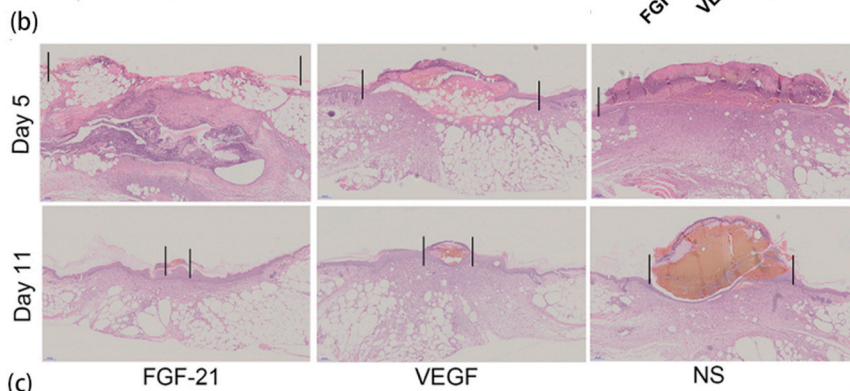
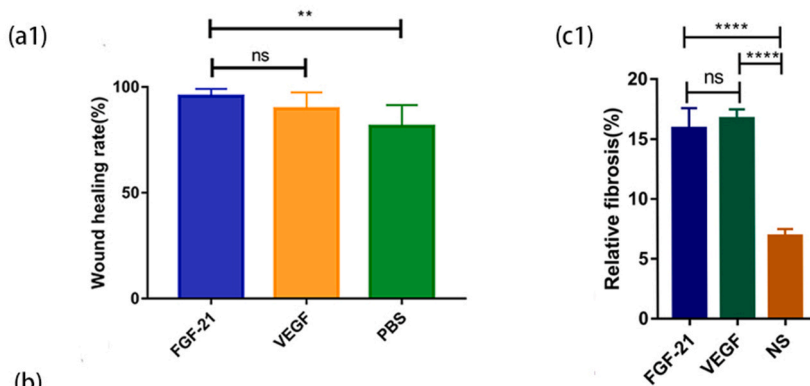
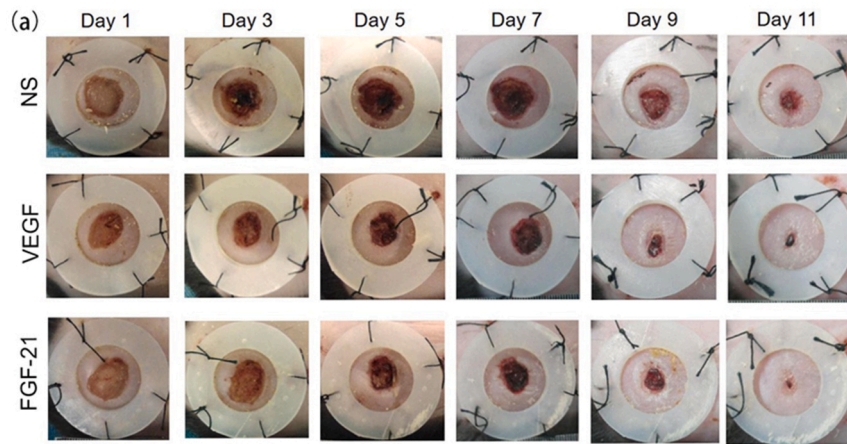
The effect of FGF-21 on HUVEC cell death in a high glucose environment was investigated using annexin V double staining with fluorescein isothiocyanate (FITC) and propidium iodide (PI). Flow cytometry was performed to determine the proportion of apoptotic cells when 30 mM glucose or FGF-21 was introduced. As we expected, HUVEC cells in 30 mM glucose showed significantly increased early (PI: negative/annexin V: positive) and late apoptosis (PI: positive/annexin V: positive cells) compared to the control group, and this situation was ameliorated by FGF-21. The percentages of early and late apoptotic cells in HUVEC are $2.48 \pm 0.43 \%$ (Control), $5.93 \pm 0.65 \%$ (30 mM glucose), $2.87 \pm 0.21 \%$ (30 mM glucose + FGF-21 group) (Fig. 1D). The endothelial tube-formation rate for the control group was $99.42 \% \pm 10.31 \%$, for the 30 mM glucose group was $86.21 \% \pm 3.12 \%$, and for the 30 mM glucose + FGF-21 group was $88.92 \% \pm 9.31 \%$. Which demonstrated that the angiogenesis ability in HUVEC cells was fully restored when FGF-21 was used under high glucose condition (Fig. 1E). These findings revealed that FGF-21 promoted cell proliferation, migration, apoptosis, and tube formation in vivo under high glucose stress. The above study utilized one-way ANOVA analysis.

3.2. Morphological changes of cells in transmission electron microscopy

Transmission Electron Microscopy was then utilized to investigate the effect of FGF-21 on the morphological structure of HUVEC cells in a high glucose environment. Both 30 mM and 60 mM glucose addition showed significantly enhanced cell swelling. In addition, endothelial cells treated with varied doses of glucose showed larger and swelling mitochondria, as well as blurring mitochondria cristae architecture. Besides, 60 mM glucose accumulates a high amount of lipid droplets in cells, which is a part of the cellular stress response to a high glucose environment. Moreover, the cell membrane perforation was observed in the 60 mM glucose group. This typical pyroptosis morphology demonstrated that as the concentration of glucose increases, endothelial cells present as pyroptosis and inflammation, which may serve as one major cause of difficulty in wound healing. However, FGF-21 treatment can completely restore mitochondrial damage and morphological changes in endothelial cells caused by glucose (Fig. 2).

3.3. FGF-21 inhibited NF- κ B p65 and NLRP3 inflammasome activation in vitro

Some important molecules of pyroptosis were discovered using qRT-PCR and Western blot analysis to elucidate the underlying mechanism of FGF-21 in vitro. We first tested the inflammation relative mRNA expression levels of NF- κ B p65, NLRP3 and IL-1 β in different groups of endothelial cells by RT-PCR. The results demonstrated that compared with the control group, NF- κ B p65, NLRP3, and IL-1 β expression level were markedly increased in the 30 mM glucose group, which was reversed by the FGF-21 treatment (Fig. 3A). Subsequently, consistent with the qRT-PCR results, Western blot analysis showed that FGF-21 significantly inhibited glucose-induced pyroptosis protein expression, including NF- κ B p65, GSDMD, NLRP3, Cleaved-caspase 1, IL-1 β under glucose overload



(caption on next page)

Fig. 4. FGF-21 promotes wound healing in db/db mice. (a) Images of skin wound sites on db/db mice taken 1, 3, 5, 7, and 11 days post wounding, Divided in NS (injected 0.5 ml 0.9 % NaCl subcutaneously), VEGF (inject 5ug/kg VEGF subcutaneously) and FGF-21(inject 5 μ g/kg FGF-21 subcutaneously) group; (b) H&E-stained sections of db/db mice (Day 11) of wound closure, 100 \times ; (c) The Masson staining of db/db mice (Day 11) of wound closure, 400 \times and quantitative analysis of relative fibrosis.(ns: P > 0.05; *P < 0.05; **P < 0.01; ***P < 0.001).

conditions (Fig. 3B–i). However, for the NIH-3T3 cell, we didn't observe increased protein levels of Cleaved-caspase 1, GSDMD, NLPR3, and IL-1 β in the 30 mM glucose group. Despite that, FGF-21 lowers Cleaved-caspase 1, GSDMD, and NLPR3 expression in NIH-3T3 cells, indicating that FGF-21 has an inhibitory effect on inflammation-related reactions (Fig. 3B–ii). The quantification and normalization results of the protein band data are shown in (Fig. 6d).

Also, higher lactate dehydrogenase (LDH) levels were observed in both HUVEC and NIH-3T3 cells treated with 30 mM glucose. Following that, FGF-21 therapy significantly restored the pyroptosis-related inflammatory response (Fig. 3c). These results indicated that FGF-21 may suppress glucose-induced pyroptosis of cells by targeting NF- κ B p65/NLRP3/Caspase1 pathway.

Furthermore, considering the protective effect of FGF-21 on mitochondrial morphology under high glucose condition, we also performed qRT-PCR to detect the mRNA expression level of FIS1, DRP1, OPA1, and MFN1, which are proteins related to the fusion and fission of mitochondrial. The results indicated that the expression of the fission-related gene FIS1 increased in high glucose conditions, and decreased after FGF-21 treatment. Both OPA1 and MFN1 expression levels were reduced in the 30 mM glucose group and then restored by FGF-21 treatment. However, the mRNA level of DRP1 in the three groups remained no significant difference. (Fig. 3D–G).

3.4. FGF-21 promotes wound healing in db/db mice

To explore the role of FGF-21 during diabetic skin wound healing, we created full-thickness punch wounds in the back skin of db/db mice on both sides of the body. Then different groups were treated with subcutaneous injection of 5ug/kg FGF-21, 5ug/kg VEGF and 5ug/kg 0.9 % saline, respectively. Skin wound biopsies were performed and the wound closure rate was analyzed using macroscopic images. On day 11, the wound closure rate in both FGF-21 and VEGF treatment groups was considerably higher than in 0.9 % saline-treated mice. The closure rates for the FGF-21 group were 94.31 % \pm 3.44 %, for the VEGF group were 87.53 % \pm 6.21 %, and for the saline group were 78.35 % \pm 7.33 %. (Fig. 4A and 5B). The distance between the wound margins (wound width) was substantially lower, and granulation tissue formation was enhanced in both the FGF-21 and VEGF groups, according to HE staining (Fig. 4B). Additionally, Masson staining was utilized to assess collagen deposition; the collagen deposition of the VEGF and FGF-21 groups was greater than that of the 0.9 % saline group (Fig. 4C). While there was no significant difference in the healing rate, matured granulation tissue, and collagen deposition of the FGF-21 group compared to the VEGF-treated group, this suggests that FGF-21 performs the same pro-healing roles as VEGF in diabetic wound healing.

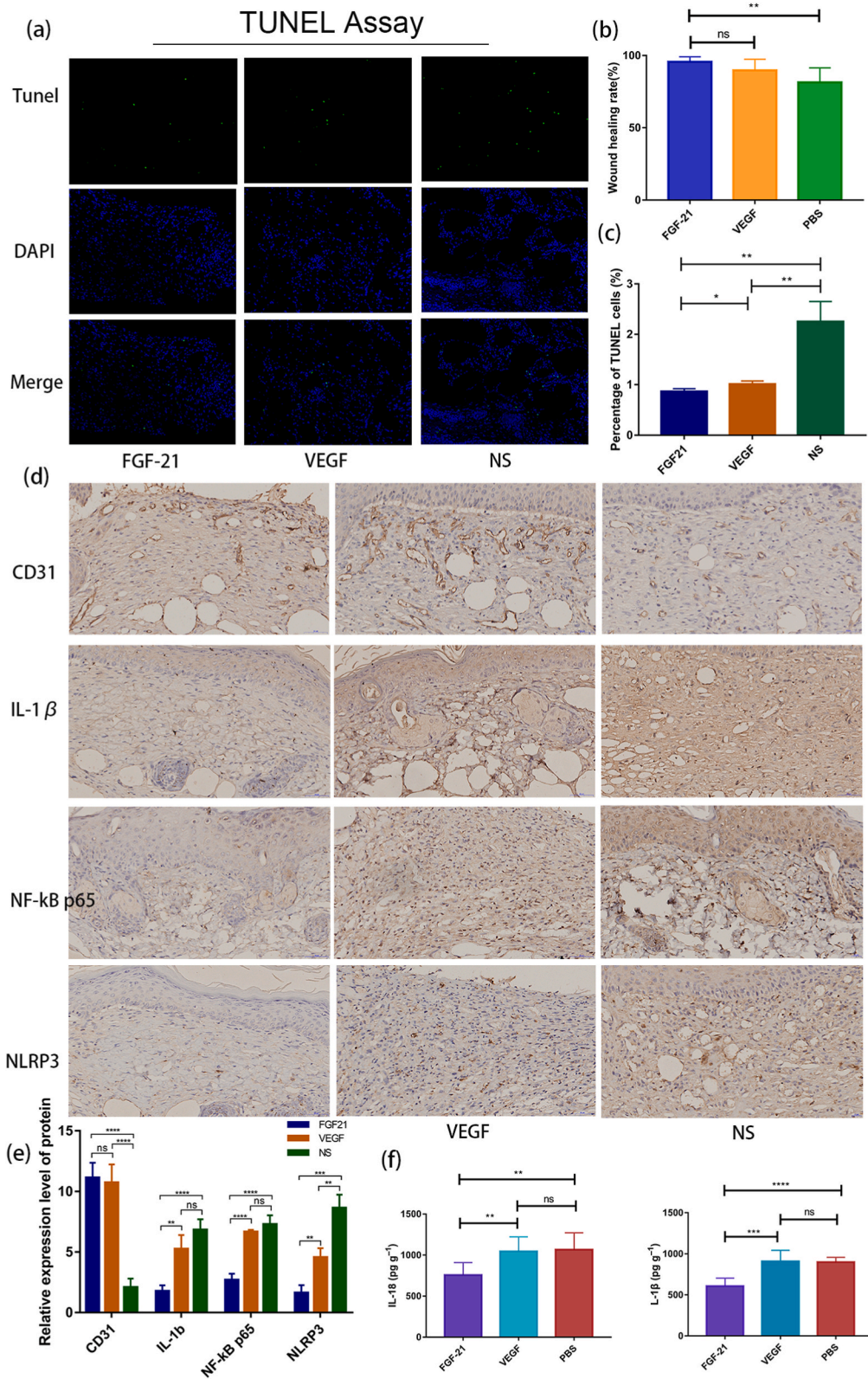
3.5. FGF-21 alleviate cell death and inflammatory response in diabetic wound

To verify the pyroptosis level in diabetic wounds in vivo, the results of cell death evaluation by the TUNEL staining in wound skin tissue were consistent with those in cells. It's also worth noting that FGF-21 and VEGF treatments both reduced the proportion of TUNEL positive cells, with FGF-21 providing more protection from cell death (Fig. 5A and C). In order to explore the specific mechanism of the effect of FGF-21 in the diabetic wound, IHC and ELISA were performed to detect the expression of pyroptosis-related proteins in wound skin on day 11. We discovered that there was no significant difference in skin CD31 expression between the FGF-21 and VEGF-treated groups, indicating that FGF-21 had the same impact on stimulating angiogenesis in diabetic wounds as VEGF. IHC analysis of IL-1 β , NF κ b-65 and NLRP3 was also performed to confirm the anti-inflammatory effect of FGF-21 on diabetic wounds. The results showed that the expression of IL-1 β and NF κ b-p65 was considerably lower in the 30 mM glucose+200 ng/ml FGF-21 group as compared to the VEGF and normal saline groups. In addition, NLRP3 expression was lower in the VEGF group compared to the control group, although it was lower in the FGF group more than in the VEGF group (Fig. 5D–E). Furthermore, the results of IL-1 β and IL-18 expression in diabetic wound tissues detected by ELISA were consistent with those indicators of inflammation in the corresponding groups (Fig. 5F). These results suggest that FGF-21 offers stronger protections than VEGF for diabetic wounds from developing inflammation injury.

4. Discussion

Diabetic non-healing wound is a major healthcare expense among chronic wounds worldwide due to their progression [8]. Early detection and effective treatment techniques are crucial, and understanding the mechanisms of key regulatory molecules involved in various pathophysiological variables throughout the healing process is necessary. Recent studies have identified fibroblast growth factor-21 (FGF-21) as a promising therapeutic target for diabetic wound healing, given its low expression levels in normal skin but significant increases during the re-epithelialization phase following damage in normal wound healing [25].

Numerous studies have shown that FGF-21 can affect various signaling pathways related to the development of diabetes and its complications. For instance, FGF-21 has been found to attenuate type 2 diabetes-induced blood-brain barrier damage by upregulating NF-E2-related factor-2 (NRF2) and activating the FGFR1/Keap1/Nrf2 pathway [26], as well as ameliorating diabetes-induced aortic endothelial cell dysfunction in mice by activating the CAMKK2/AMPK signaling pathway [27]. Recent research suggests that FGF-21 also plays a crucial role in regulating pyroptosis, preventing oxidized low-density lipoprotein-induced pyroptosis in human endothelial



(caption on next page)

Fig. 5. Evaluation of cell death rate (TUNEL staining) and inflammatory indicators in diabetic wound. (a) Representative images of TUNEL staining (magnification $\times 400$) in diabetic wound on 11 day of each group; (b) Quantitative analysis of the wound healing rate in different group; (c) TUNEL positive cells were counted and statistics analysis was performed in each group; (d) Immunohistochemical staining of CD31, IL-1 β , NF- κ B p65 and NLRP3 in diabetic wound in each group, 400 \times ; (e) Statistical result of immunohistochemical staining; (f) ELISA assay for IL-1 β and IL-18 in wound tissues in each group. (ns: $P > 0.05$; * $P < 0.05$; ** $P < 0.01$; *** $P < 0.001$).

cells by regulating the TET2-UQCRC1-ROS pathway [28]. In this study, our results indicate that FGF-21 treatment restored hyperglycemic damage on endothelial cell proliferation, migration, and tube-forming ability while reducing cell death rates, reflecting its protective effect on endothelial function in diabetic wounds. Encapsulating FGF-21 and dimethyldigua in ROS hydrogel has also been proposed as a potential new drug delivery system for diabetic wounds, with significant therapeutic effects observed in animal experiments [29]. These findings highlight the potential of innovative drug delivery systems for FGF-21 to enhance its therapeutic efficacy in treating diabetic wounds.

Cell pyroptosis is followed by cell penetration swelling and "hole punching" activity of the cell membrane, resulting in the release of cellular contents such as LDH, as well as intracellular inflammatory factors including IL-1 β and IL-18 [30,31]. Furthermore, the transcription factor NF- κ B plays an indispensable role in the activation of the NLRP3-inflammasome and regulating caspase-1 [32,33]. After high-glucose treatment, NF- κ B silencing was reported to diminish the expression of the NLRP3 inflammasome in mouse mesenchymal cells (MCs) [34]. Moreover, inhibition of NF- κ B was also found to reduce NLRP3 inflammasome activation in myocardial cells of type 2 diabetic rats [35]. Our study showed that with increasing glucose concentration, endothelial cell death rates increased, accompanied by typical pyroptosis morphology and LDH release. The expression of several inflammatory factors, including NF- κ B-p65, NLRP3, Cleaved-caspase 1, GSDMD, and mature IL-1 β , also increased in endothelial cells under high glucose conditions. However, FGF-21 treatment completely restored this inflammatory response. These findings demonstrate that pyroptosis is implicated in the pathological process of glucose-induced endothelial dysfunction, and FGF-21 may reduce the classical pyroptosis pathway activation during diabetic wound healing.

However, in NIH-3T3 cells, high glucose treatment did not lead to obvious pyroptosis manifestations. Nevertheless, FGF-21 treatment reduced the release of LDH and the expression of inflammation factors including caspase-1 and NLRP3, confirming its beneficial effect on inflammation control in wound healing-related cells. Notably, using db/db mice as animal model, we found that FGF-21 effectively promoted wound healing. Although there was no significant difference in wound healing rate between the FGF-21-treated group and the positive control group (VEGF-treated), the FGF-21-treated group showed a slightly higher rate. Moreover, H&E, Masson, and IHC staining for CD31 showed that FGF-21 and VEGF therapy had similar effects on stimulating angiogenesis and collagen deposition throughout the diabetic wound healing process. However, IHC analysis of inflammatory factors including NF- κ B p65, IL-1 β , and NLRP3 suggested that FGF-21 therapy more effectively inhibited inflammation than VEGF or normal saline treatment. The result of the TUNEL assay in wound tissues of db/db mice in different groups is consistent with this observation. After the completion of the overall experiment, we conducted an additional FGF-21 gene knockout experiment on HUVEC cells, categorizing the cells into four groups: control group, high-glucose group, FGF-21 knockout group, and FGF-21 knockout + high-glucose group. We compared the differences in proliferation and migration rates between the FGF-21 knockout group and the control group. The proliferation and migration rates of FGF-21 knockout cells were found to be lower than those of the control group cells in both high-glucose and non-high-glucose environments, and the differences were statistically significant shown in (Fig. 6 a-c). Our result suggested that FGF-21 may serve as a more suitable factor than VEGF for treating inflammatory diseases treatment such as diabetic wound.

Moreover, considering the protective effect of FGF-21 on mitochondrial structure in a high glucose environment detected by TEM, we performed RT-PCR to decipher the underlying mechanism. Our results indicated that under high glucose conditions, the expression of the fission-related protein Fis1 increased dramatically and was reversed by FGF-21 treatment, which is consistent with the mitochondrial deformation and conservation observed in TEM. Additionally, the mRNA levels of fusion-related proteins Mfn1 and Opa1, which improve mitochondrial functions, biogenesis, and angiogenesis, [36–38], were both decreased under hyperglycemic conditions and considerably increased following FGF-21 treatment. This result could offer a possible explanation for why FGF-21 promotes the angiogenesis function of endothelial cells.

Overall, our findings first revealed a novel molecular mechanism involving FGF-21 and the pyroptosis pathway that underpins diabetic wound healing. Compared to VEGF, FGF-21 may represent a superior candidate for treating non-healing diabetic wounds due to its unique therapeutic effect of inhibiting the inflammatory response. Understanding these mechanisms and physiological functions of FGF-21 could help facilitate the development of new approaches for mitigating the diabetes-induced impairment in wound healing.

In this study, we must acknowledge the presence of certain limitations. Firstly, the sample size was relatively small, which may have constrained the generalizability and reliability of the results. Secondly, due to experimental constraints and budget limitations, we were unable to conduct comprehensive WB validation and animal gene knockout validation. These limitations could impact our interpretation and conclusions drawn from the results. To enhance future research, we plan to increase the sample size. Additionally, future studies could further investigate the FGF-21 gene knockout rat model to gain a deeper understanding of its mechanism in wound healing. Furthermore, applying for clinical trials will help validate the applicability of laboratory results in clinical practice.

Data access statement

Data available on request from the authors.

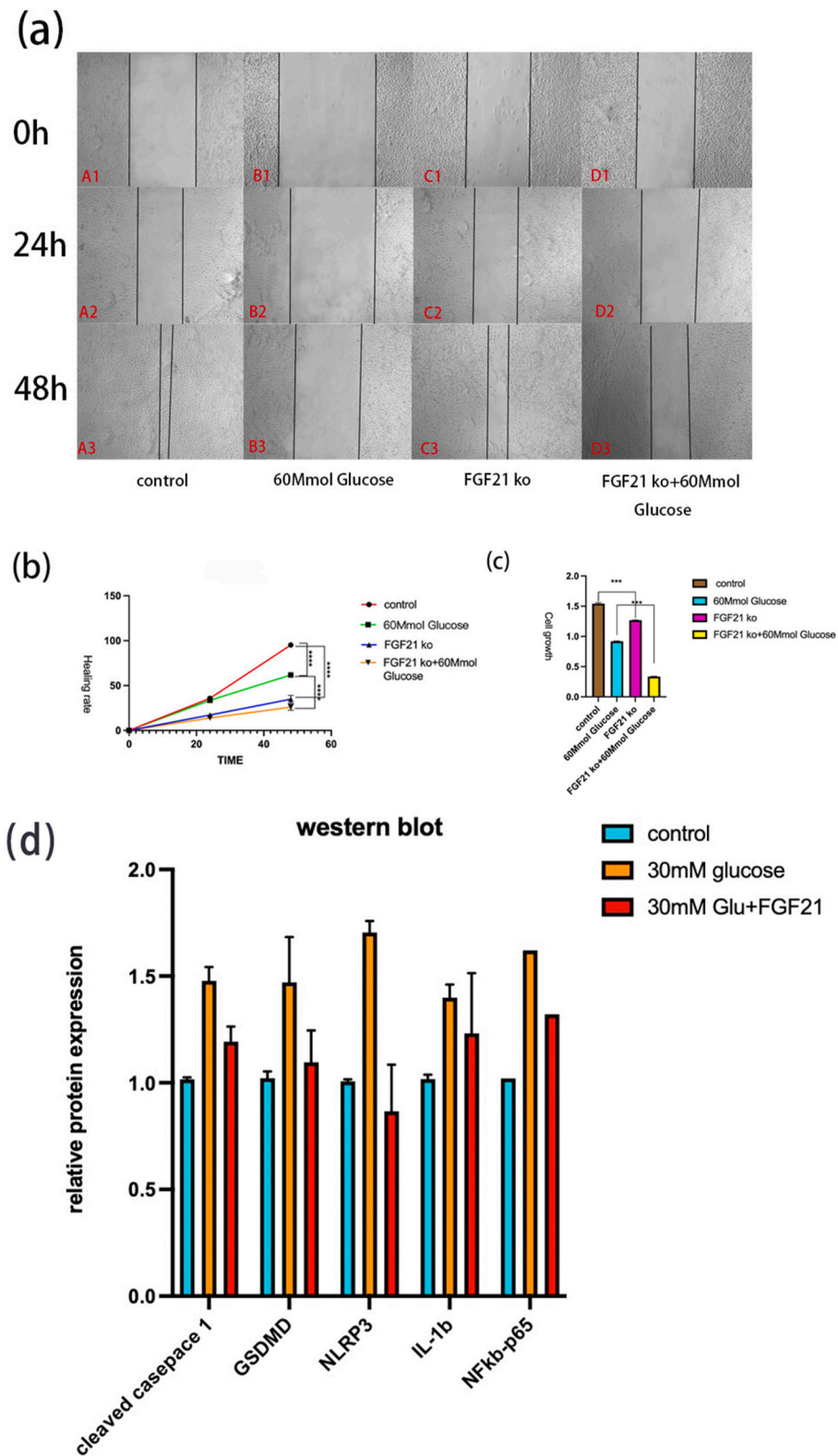


Fig. 6.

CRedit authorship contribution statement

Zheling Li: Methodology, Formal analysis. **Xiaohui Qiu:** Writing – original draft, Methodology, Formal analysis. **Gaopeng Guan:** Resources. **Ke Shi:** Software. **Shuyue Chen:** Investigation. **Jiangjie Tang:** Methodology. **Muzhang Xiao:** Software. **Shijie Tang:** Methodology. **Yu Yan:** Funding acquisition, Haihong Li, Methodology. **Jianda Zhou:** Methodology, Investigation, Funding acquisition, Methodology. **Huiqing Xie:** Methodology.

Declaration of competing interest

The authors declare the following financial interests/personal relationships which may be considered as potential competing interests: Jianda Zhou reports was provided by Xiangya Third Hospital of Central South University. Jianda Zhou reports a relationship with Xiangya Third Hospital of Central South University that includes: employment. Jianda Zhou has patent pending to Jianda Zhou. No conflicts of interest that require special declaration If there are other authors, they declare that they have no known competing financial interests or personal relationships that could have appeared to influence the work reported in this paper.

Appendix A. Supplementary data

Supplementary data to this article can be found online at <https://doi.org/10.1016/j.heliyon.2024.e30022>.

Abbreviations

MMPs	matrix metal loproteinases
DFU	diabetic foot ulceration
GFs	growth factors
VEGF	vascular endothelial GF
FGF	fibroblast GF
EGF	epidermal GF
TGF- β	transforming GF- β
PDGF	platelet-derived growth factor
T2 DM	type 2 diabetes mellitus
CCK8	Cell Counting Kit-8 assay
TEM	Transmission electron microscope cell morphology observation
qRT-PCR	RNA isolation and quantitative real-time PCR
ELISA	Enzyme-linked immunosorbent assay

References

- [1] C.L. Baum, C.J. Arpey, Normal cutaneous wound healing: clinical correlation with cellular and molecular events, *Dermatol. Surg.* : official publication for American Society for Dermatologic Surgery [et al] 31 (6) (2005) 674–686. ; discussion 686.
- [2] H. Galkowska, W.L. Olszewski, U. Wojewodzka, G. Rosinski, W. Karnafel, Neurogenic factors in the impaired healing of diabetic foot ulcers, *J. Surg. Res.* 134 (2) (2006) 252–258.
- [3] N. Amin, J. Doupis, Diabetic foot disease: from the evaluation of the "foot at risk" to the novel diabetic ulcer treatment modalities, *World J. Diabetes* 7 (7) (2016) 153–164.
- [4] R.F. Diegelmann, M.C. Evans, Wound healing: an overview of acute, fibrotic and delayed healing, *Front. Biosci.* : J. Vis. Literacy 9 (2004) 283–289.
- [5] S.A. Eming, P. Martin, M. Tomic-Canic, Wound repair and regeneration: mechanisms, signaling, and translation, *Sci. Transl. Med.* 6 (265) (2014) 265r266.
- [6] A.J. Singer, R.A. Clark, Cutaneous wound healing, *N. Engl. J. Med.* 341 (10) (1999) 738–746.
- [7] I. Eleftheriadou, A. Tentolouris, P. Grigoropoulou, D. Tsilingiris, I. Anastasiou, A. Kokkinos, D. Perrea, N. Katsilambros, N. Tentolouris, The association of diabetic microvascular and macrovascular disease with cutaneous circulation in patients with type 2 diabetes mellitus, *J. Diabetes Complicat.* 33 (2) (2019) 165–170.
- [8] S. Akhtar, N. Schaper, J. Apelqvist, E. Jude, A review of the Eurodiab studies: what lessons for diabetic foot care? *Curr. Diabetes Rep.* 11 (4) (2011) 302–309.
- [9] X. Li, C. Jiang, J. Zhao, Human endothelial progenitor cells-derived exosomes accelerate cutaneous wound healing in diabetic rats by promoting endothelial function, *J. Diabetes Complicat.* 30 (6) (2016) 986–992.
- [10] Y. Heun, M. Anton, A. Pfeifer, C. Plank, U. Pohl, H. Mannell, Lentiviral Magnetic Targeting of SHP-2 Locally Governs HIF-1a Dependent Wound Healing Angiogenesis in Vivo, 2017.
- [11] M. Rodrigues, N. Kosaric, C.A. Bonham, G.C. Gurtner, Wound healing: a cellular perspective, *Physiol. Rev.* 99 (1) (2019) 665–706.
- [12] M. Petkovic, A.E. Sørensen, E.C. Leal, E. Carvalho, L.T. Dalgaard, Mechanistic actions of microRNAs in diabetic wound healing, *Cells* 9 (10) (2020).
- [13] J. Gao, J. Zhang, L. Xia, X. Liang, W. Ding, M. Song, L. Li, Z. Jia, Up-regulation of caveolin 1 mediated by chitosan activates Wnt/ β -catenin pathway in chronic refractory wound diabetic rat model, *Bioengineered* 13 (1) (2022) 1388–1398.
- [14] M. Chang, T.T. Nguyen, Strategy for treatment of infected diabetic foot ulcers, *Acc. Chem. Res.* 54 (5) (2021) 1080–1093.
- [15] M. Zubair, J. Ahmad, Role of growth factors and cytokines in diabetic foot ulcer healing: a detailed review, *Rev. Endocr. Metab. Disord.* 20 (2) (2019) 207–217.
- [16] G. Kolumam, X. Wu, W.P. Lee, J.A. Hackney, J. Zavala-Solorio, V. Gandham, D.M. Danilenko, P. Arora, X. Wang, W. Ouyang, IL-22R ligands IL-20, IL-22, and IL-24 promote wound healing in diabetic db/db mice, *PLoS One* 12 (1) (2017) e0170639.
- [17] E. Mahdipour, A. Sahebkar, The role of recombinant proteins and growth factors in the management of diabetic foot ulcers: a systematic review of randomized controlled trials, *J. Diabetes Res.* 2020 (2020) 6320514.

- [18] J. Moura, A. Sørensen, E.C. Leal, R. Svendsen, L. Carvalho, R.J. Willemoes, P.T. Jørgensen, H. Jenssen, J. Wengel, L.T. Dalgaard, et al., microRNA-155 inhibition restores Fibroblast Growth Factor 7 expression in diabetic skin and decreases wound inflammation, *Sci. Rep.* 9 (1) (2019) 5836.
- [19] S. Rühl, K. Shkarina, B. Demarco, R. Heilig, J.C. Santos, P. Broz, ESCRT-dependent membrane repair negatively regulates pyroptosis downstream of GSDMD activation, *Science (New York, NY)* 362 (6417) (2018) 956–960.
- [20] J. Shi, Y. Zhao, K. Wang, X. Shi, Y. Wang, H. Huang, Y. Zhuang, T. Cai, F. Wang, F. Shao, Cleavage of GSDMD by inflammatory caspases determines pyroptotic cell death, *Nature* 526 (7575) (2015) 660–665.
- [21] Y. Kim, W. Wang, M. Okla, I. Kang, R. Moreau, S. Chung, Suppression of NLRP3 inflammasome by γ -tocotrienol ameliorates type 2 diabetes, *J. Lipid Res.* 57 (1) (2016) 66–76.
- [22] D. Wu, Z.B. Yan, Y.G. Cheng, M.W. Zhong, S.Z. Liu, G.Y. Zhang, S.Y. Hu, Deactivation of the NLRP3 inflammasome in infiltrating macrophages by duodenal-jejunal bypass surgery mediates improvement of beta cell function in type 2 diabetes, *Metab. Clin. Exp.* 81 (2018) 1–12.
- [23] F. Yang, Y. Qin, Y. Wang, A. Li, J. Lv, X. Sun, H. Che, T. Han, S. Meng, Y. Bai, et al., LncRNA KCNQ1OT1 mediates pyroptosis in diabetic cardiomyopathy, *Cell. Physiol. Biochem. : international journal of experimental cellular physiology, biochemistry, and pharmacology* 50 (4) (2018) 1230–1244.
- [24] P. Sa-Nguanmoo, P. Tanajak, S. Kerdphoo, T. Jaiwongkam, X. Wang, G. Liang, X. Li, C. Jiang, W. Pratchayasakul, N. Chattipakorn, et al., FGF21 and DPP-4 inhibitor equally prevents cognitive decline in obese rats, *Biomedicine & pharmacotherapy = Biomedecine & pharmacotherapie* 97 (2018) 1663–1672.
- [25] X. Chen, G. Tong, J. Fan, Y. Shen, N. Wang, W. Gong, Z. Hu, K. Zhu, X. Li, L. Jin, et al., FGF21 promotes migration and differentiation of epidermal cells during wound healing via SIRT1-dependent autophagy, *Br. J. Pharmacol.* 179 (5) (2022) 1102–1121.
- [26] Z. Yu, L. Lin, Y. Jiang, I. Chin, X. Wang, X. Li, E.H. Lo, X. Wang, Recombinant FGF21 protects against blood-brain barrier leakage through Nrf2 upregulation in type 2 diabetes mice, *Mol. Neurobiol.* 56 (4) (2019) 2314–2327.
- [27] L. Ying, N. Li, Z. He, X. Zeng, Y. Nan, J. Chen, P. Miao, Y. Ying, W. Lin, X. Zhao, et al., Fibroblast growth factor 21 Ameliorates diabetes-induced endothelial dysfunction in mouse aorta via activation of the CaMKK2/AMPK α signaling pathway, *Cell Death Dis.* 10 (9) (2019) 665.
- [28] J.J. Chen, J. Tao, X.L. Zhang, L.Z. Xia, J.F. Zeng, H. Zhang, D.H. Wei, Y.C. Lv, G.H. Li, Z. Wang, Inhibition of the ox-LDL-induced pyroptosis by FGF21 of human umbilical vein endothelial cells through the TET2-UQCRC1-ROS pathway, *DNA Cell Biol.* 39 (4) (2020) 661–670.
- [29] H. Zhu, J. Xu, M. Zhao, H. Luo, M. Lin, Y. Luo, Y. Li, H. He, J. Wu, Adhesive, injectable, and ROS-responsive hybrid polyvinyl alcohol (PVA) hydrogel co-delivers metformin and fibroblast growth factor 21 (FGF21) for enhanced diabetic wound repair, *Front. Bioeng. Biotechnol.* 10 (2022) 968078.
- [30] J. Shi, Y. Zhao, Y. Wang, W. Gao, J. Ding, P. Li, L. Hu, F. Shao, Inflammatory caspases are innate immune receptors for intracellular LPS, *Nature* 514 (7521) (2014) 187–192.
- [31] Y. Wang, W. Gao, X. Shi, J. Ding, W. Liu, H. He, K. Wang, F. Shao, Chemotherapy drugs induce pyroptosis through caspase-3 cleavage of a gasdermin, *Nature* 547 (7661) (2017) 99–103.
- [32] S. Vallabhapurapu, M. Karin, Regulation and function of NF-kappaB transcription factors in the immune system, *Annu. Rev. Immunol.* 27 (2009) 693–733.
- [33] K. Schroder, R. Zhou, J. Tschopp, The NLRP3 inflammasome: a sensor for metabolic danger? *Science (New York, NY)* 327 (5963) (2010) 296–300.
- [34] H. Yi, R. Peng, L.Y. Zhang, Y. Sun, H.M. Peng, H.D. Liu, L.J. Yu, A.L. Li, Y.J. Zhang, W.H. Jiang, et al., LincRNA-Gm4419 knockdown ameliorates NF- κ B/NLRP3 inflammasome-mediated inflammation in diabetic nephropathy, *Cell Death Dis.* 8 (2) (2017) e2583.
- [35] B. Luo, B. Li, W. Wang, X. Liu, Y. Xia, C. Zhang, M. Zhang, Y. Zhang, F. An, NLRP3 gene silencing ameliorates diabetic cardiomyopathy in a type 2 diabetes rat model, *PLoS One* 9 (8) (2014) e104771.
- [36] T. Vezza, P. Díaz-Pozo, F. Canet, A.M. de Marañón, Z. Abad-Jiménez, C. García-Gargallo, I. Roldan, E. Solá, C. Bañuls, S. López-Domènech, et al., The role of mitochondrial dynamic dysfunction in age-associated type 2 diabetes, *The world journal of men's health* 40 (3) (2022) 399–411.
- [37] A. Chehaitly, A.L. Guihot, C. Proux, L. Grimaud, J. Aurrière, B. Legourellec, J. Rivron, E. Vessieres, C. Tétaud, A. Zorzano, et al., Altered mitochondrial opa1-related fusion in mouse promotes endothelial cell dysfunction and atherosclerosis, *Antioxidants* 11 (6) (2022).
- [38] R. Zou, W. Shi, J. Qiu, N. Zhou, N. Du, H. Zhou, X. Chen, L. Ma, Empagliflozin attenuates cardiac microvascular ischemia/reperfusion injury through improving mitochondrial homeostasis, *Cardiovasc. Diabetol.* 21 (1) (2022) 106.